Accurately representing the Coriolis effect on gravity waves

R. Michael Jones[a], Alfred J. Bedard Jr.[a], Xinzhao Chu[a], Ian Geraghty[a], Jian Zhao[a], & others?[a]

[a]*Cooperative Institute for Research in Environmental Sciences, University of Colorado, Boulder, Colorado 80309-0216, U.S.A.*

Abstract

The usual formula for the acoustic-gravity wave dispersion relation (that depends on only the vertical component of the Earth's angular velocity in the Coriolis force) gives the correct low-frequency cut off, but including all components of the Earth's angular velocity gives more accurate propagation calculations in some cases.

Keywords:

1. Introduction

Gravity waves have been measured in Antarctica that have periods ranging from 3 to 10 hours (Chu et al., 2011; Chen et al., 2013, 2016; Zhao et al., 2017). To correctly interpret gravity wave measurements at such low frequencies with ray tracing calculations requires an accurate representation of the effect of Coriolis force on the propagation.

Although the usual dispersion relation (Eckart, 1960, eq. (51-2), p. 125) (Gossard and Hooke, 1975, eq. (23-7), p. 112) that includes the effect of only the vertical component of the Earth's angular velocity on the Coriolis force[1] gives the correct low-frequency cut off for inertial gravity waves, it neglects possibly significant effects from the horizontal components of the Earth's angular velocity.

Section 2 gives the usual barotropic dispersion relation that includes only the vertical component of the Earth's angular velocity. Section 3 gives the barotropic dispersion relation that includes all components of the Earth's angular velocity. Section 4 shows a comparison of the ray paths and vertical-wavelength profiles resulting from the two versions of the dispersion relation. Section 5 presents the conclusion. Appendix A gives an approximate dispersion relation that neglects rate-of-strain and baroclinicity, but still includes the effects of all components of the Earth's angular velocity on the Coriolis force.

2. The usual dispersion relation ignores horizontal components of the Earth's angular velocity

The usual barotropic approximation to the acoustic-gravity wave dispersion relation is (Eckart, 1960, eq. (51-2), p. 125) (Gossard and Hooke, 1975, eq. (23-7), p. 112) (Jones, 2006, equation (1)):

$$(k_x^2 + k_y^2)(N^2 - \omega^2) - (\omega^2 - 4\Omega_z^2)(k_z^2 + \mathbf{k}_A^2 - \frac{\omega^2}{C^2}) = 0 \ , \quad (1)$$

where N is the Brunt-Väisälä frequency, $\omega = \sigma - \mathbf{k}\cdot\mathbf{U}$ is the intrinsic frequency, σ is the wave frequency, $\mathbf{U}$ is the background fluid velocity, $\mathbf{k}$ is the wavenumber, k_z is its vertical component, k_x and k_y are its horizontal components, Ω_z is the vertical component of the Earth's angular velocity, C is sound speed, and $\mathbf{k}_A \equiv \nabla\rho/(2\rho)$, where ρ is density.

Because the main Coriolis effect on the propagation of gravity waves is to give a low-frequency cutoff, and because that cutoff is correctly given by an approximation that neglects the effects of the horizontal components of the Earth's angular velocity, it made sense to use the simpler formula (1) based on that approximation before the wide-spread use of computers to make calculations. However, when making calculations with a computer, there is less advantage of a simple formula if a more accurate formula can give better results.

3. Including all components of the Earth's angular velocity in the Coriolis effect for the dispersion relation

Eckart (1960, sections 37-38, pp. 94-101) considers the horizontal components of the Earth's angular velocity and gives the appropriate equations, but does not calculate a dispersion relation that includes the horizontal components. Gossard and Hooke (1975, section 10, p. 50) also consider the possibility of including the horizontal components of the Earth's angular velocity in the Coriolis effect on the dispersion relation, but decide that the effect would be small. Jones (2006, equation (5)) gives a general formula for the acoustic-gravity-wave dispersion relation, including baroclinicity, rate-of-strain, and the Coriolis force (including all components of the Earth's angular velocity).

Equation (A.7), which gives an approximate dispersion relation that neglects rate-of-strain and baroclinicity, but still includes the effects of all components of the Earth's angular velocity on the Coriolis force, can be written

$$(\mathbf{k}^2 + \mathbf{k}_A^2)(N^2 - \omega^2) - \left(k_z^2 + k_A^2\right)N^2 + 4(\mathbf{k}_A \cdot \tilde{\mathbf{\Omega}})^2$$
$$+4(\mathbf{k}\cdot\tilde{\mathbf{\Omega}})^2 + 4\omega\tilde{\mathbf{\Omega}} \times \mathbf{\Gamma}\cdot\mathbf{k} + 1/C^2(\omega^4 - 4\omega^2\tilde{\mathbf{\Omega}}^2) = 0 \ , \quad (2)$$

[1] sometimes referred to as the "Shallow atmosphere" approximation (Phillips, 1966; Hickey and Cole, 1987)

where $\tilde{\mathbf{\Omega}} = \mathbf{\Omega} + \zeta/4$, $\zeta = \nabla \times \mathbf{U}$ is vorticity, and $\mathbf{\Omega}$ is the Earth's angular velocity.

Although the main Coriolis term (the first Coriolis term) in (2) agrees with the corresponding term in (1), other Coriolis terms in (2) differ because they depend on the horizontal components of the Earth's angular velocity.

4. Comparison

To compare ray paths calculated using the usual approximation (1) with the dispersion relation that includes Coriolis effects from all components of the Earth's angular velocity (2), we use a temperature profile appropriate to McMurdo, Antarctica for 29 June 2011, 20 UT, as shown in figure 1. The corresponding Brunt-Väisälä frequency profile is shown in figure 2.

Figure 3 shows the ray paths in the North-South plane neglecting horizontal components of the Earth's angular velocity using the usual dispersion relation (1). Figure 4 shows the corresponding ray paths using the dispersion relation that includes Coriolis effects from all components of the Earth's angular velocity (2). As can be seen, the rays are turned back at the same latitude in both figures 3 and 4, indicating that the low-frequency cut off for gravity waves depends only on the vertical component of the Earth's angular velocity. However, the ray paths in the two figures differ significantly, indicating that accurate calculation of ray paths requires including all components of the Earth's angular velocity in the dispersion relation.

In addition to comparing ray paths for the two versions of the dispersion relation, we can also compare profiles of vertical wavenumber and vertical wavelength. Figures 5 and 6 show a comparison of vertical-wavenumber profiles for the two versions of the dispersion relation. That they differ significantly is clear. Figures 7 and 8 show a comparison of vertical-wavelength profiles for the two versions of the dispersion relation. That they differ significantly is also clear. Figures 9 and 10 show a comparison of vertical-wavelength profiles for the two versions of the dispersion relation for a different elevation angle at the ground.

Because of horizontal gradients caused by the latitude-dependence of the Coriolis terms, there is not a one-to-one correspondence between the raypaths in figures 3 and 4 with the profiles in figures 5 through 10. However, both ray-path plots and profiles show that the turning-point height increases with elevation angle and that the turning-point heights for the dispersion relation that includes all components of the Earth's angular velocity are higher than those when the effect of the horizontal components of the Earth's angular velocity are neglected.

Although the examples presented here do not include wind, the results are similar when wind is included.

5. Conclusion

Because there can be significant differences in both ray paths and vertical-wavelength profiles between dispersion relations that include or neglect the horizontal components of the Earth's

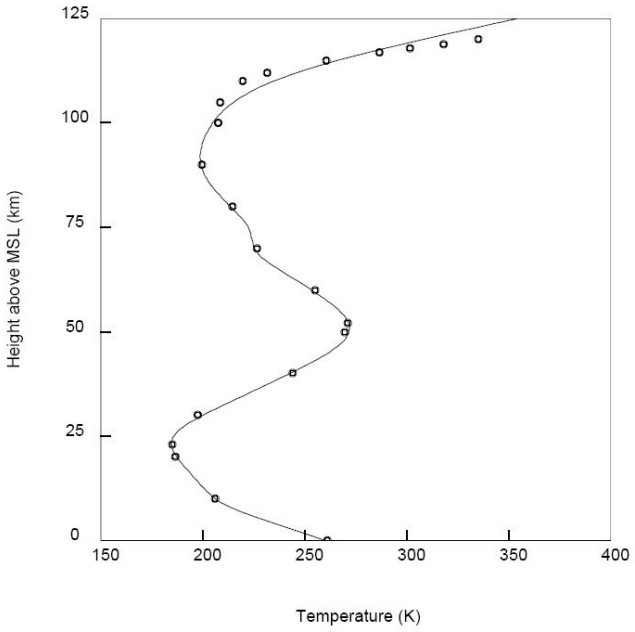

Figure 1: Temperature profile used in the ray path calculations. The circles are from the MSISE-00 model for McMurdo (77.83° S, 166.67° E) for 29 June 2011, 20 UT (NRLMSISE-00, Community Coordinated Modeling Center, 2016). The solid line is our fit to the profile that we used for the ray-path and profile calculations.

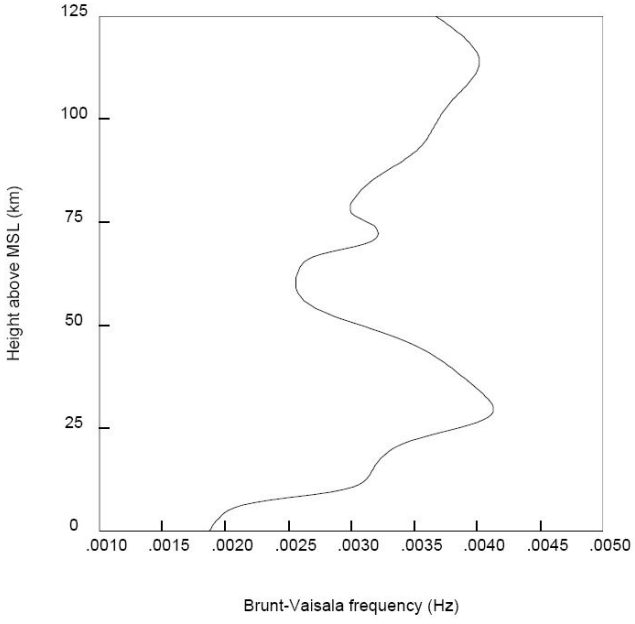

Figure 2: Brunt-Väisälä frequency profile for McMurdo (77.83° S, 166.67° E) for 29 June 2011, 20 UT corresponding to the temperature profile in figure 1.

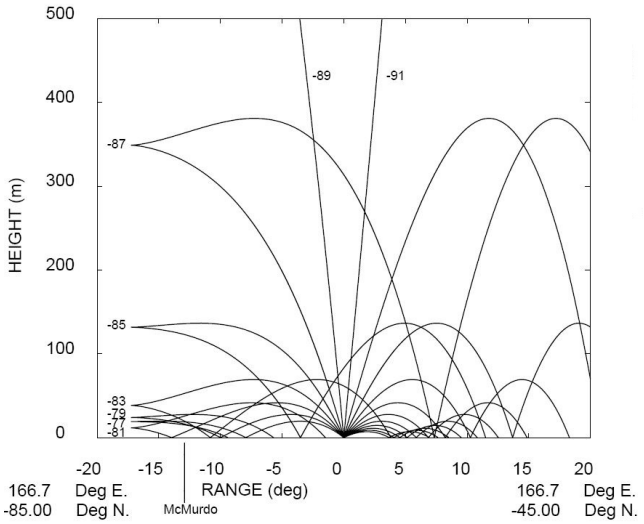

Figure 3: Ray paths in the North-South plane neglecting horizontal components of the Earth's angular velocity for the Coriolis force in the dispersion relation. The source is on the ocean surface at a latitude of 65° South and a longitude of 166.67° East. The frequency is 23 μHz. The elevation angles of transmission (wave-normal direction) of the various rays are indicated in the figure, and are relative to propagation to the South. Negative elevation angles for the wave-normal direction correspond to upward ray propagation for gravity waves. McMurdo (as indicated in the figure) is located 12.83° South of the source.

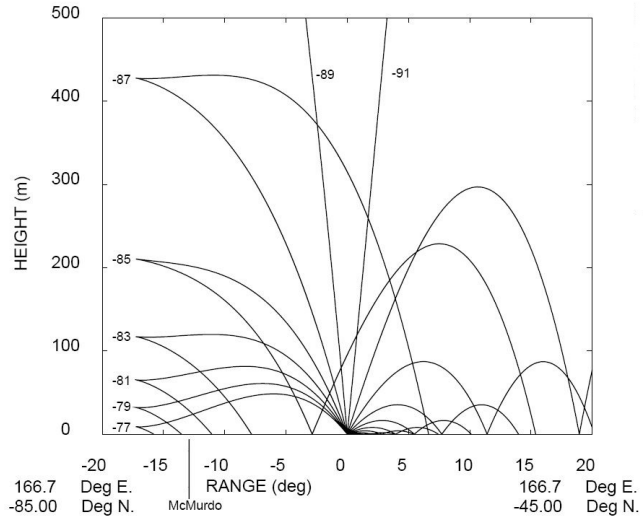

Figure 4: Ray paths in the North-South plane including all components of the Earth's angular velocity for the Coriolis force in the dispersion relation. Otherwise, conditions are as in figure 3.

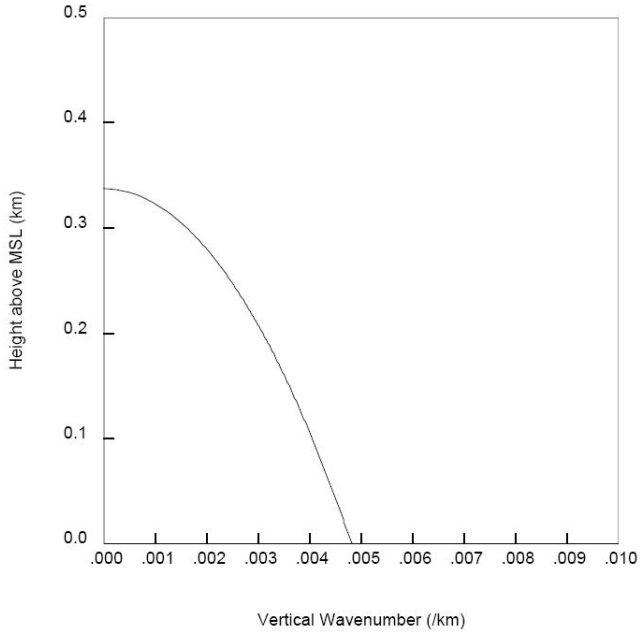

Figure 5: Vertical-wavenumber profile at McMurdo (77.83° S, 166.67° E) neglecting horizontal components of the Earth's angular velocity for the Coriolis force in the dispersion relation. The frequency is 23 μHz. Propagation is toward the South. The elevation angle at the ground is -88.7°. The wave is evanescent above the turning point, the height where the wavenumber is equal to zero.

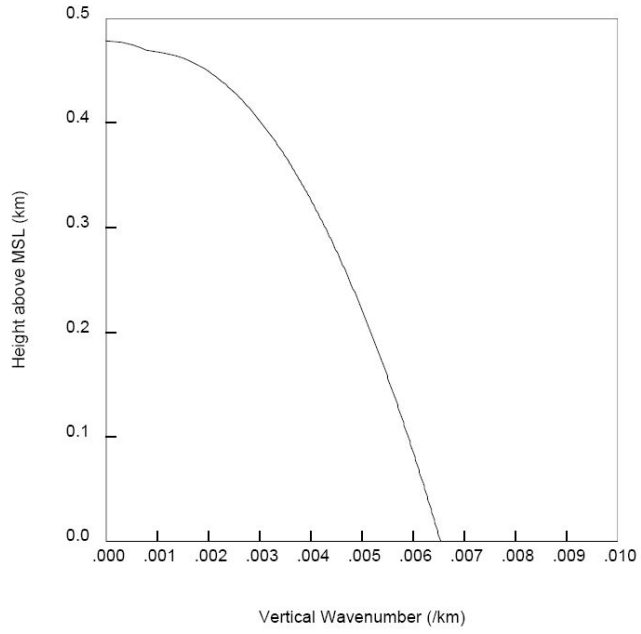

Figure 6: Vertical-wavenumber profile at McMurdo including all components of the Earth's angular velocity for the Coriolis force in the dispersion relation. The elevation angle at the ground is -88.7°. Otherwise, conditions are as in figure 5.

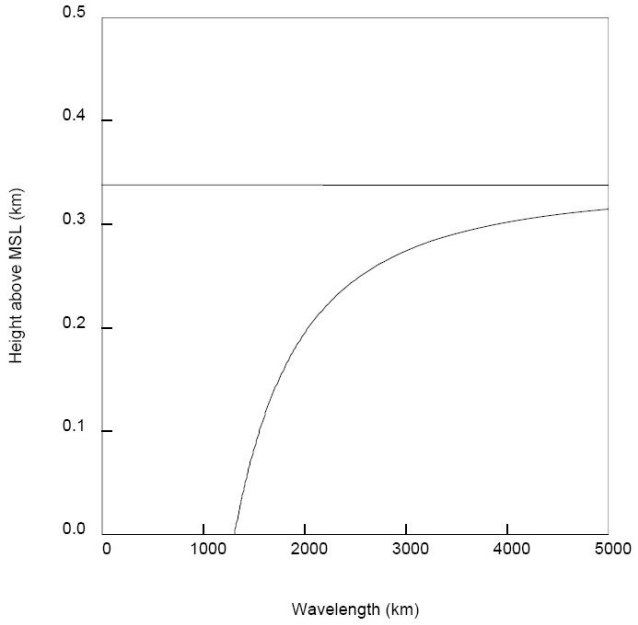

Figure 7: Vertical-wavelength profile at McMurdo neglecting horizontal components of the Earth's angular velocity for the Coriolis force in the dispersion relation. The elevation angle at the ground is -88.7°. Otherwise, conditions are as in figure 5. Because the vertical wavelength is proportional to the inverse of the vertical wavenumber, the vertical wavelength diverges at the turning point, as can be seen.

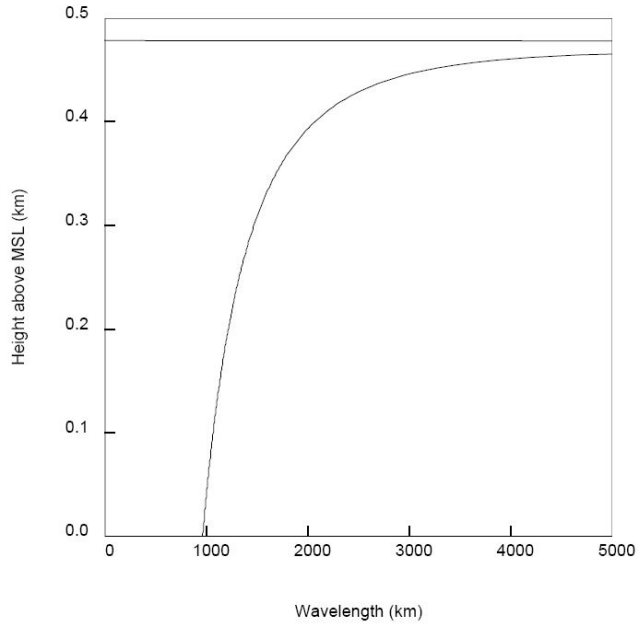

Figure 8: Vertical-wavelength profile at McMurdo including all components of the Earth's angular velocity for the Coriolis force in the dispersion relation. The elevation angle at the ground is -88.7°. Otherwise, conditions are as in figure 5.

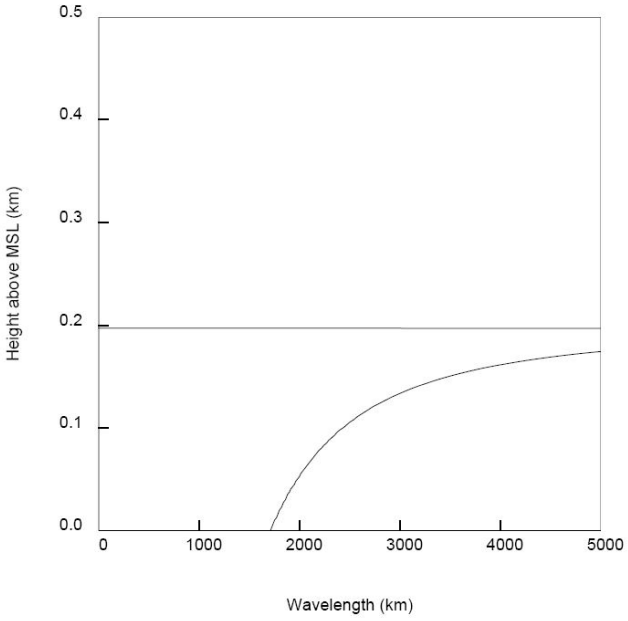

Figure 9: Vertical-wavelength profile at McMurdo neglecting horizontal components of the Earth's angular velocity for the Coriolis force in the dispersion relation. The elevation angle at the ground is -88.3°. Otherwise, conditions are as in figure 5.

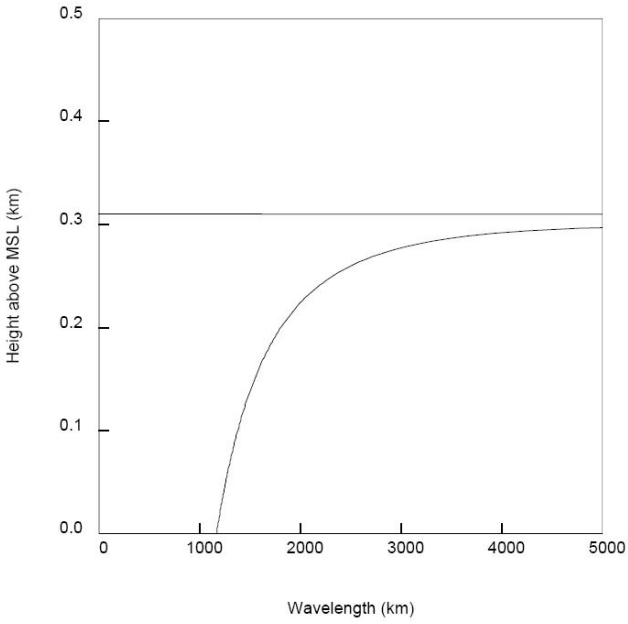

Figure 10: Vertical-wavelength profile at McMurdo including all components of the Earth's angular velocity for the Coriolis force in the dispersion relation. The elevation angle at the ground is -88.3°. Otherwise, conditions are as in figure 5.

angular velocity in the Coriolis terms, it is advisable to include all components of the Earth's angular velocity when calculating Coriolis effects on gravity-wave propagation.

Acknowledgments

This research was partially supported by the National Science Foundation (NSF) grants PLR-1246405 and AGS-1136272.

Appendix A. Dispersion relation including all components of the Earth's angular velocity.

Jones (2006, equation (5)) gives a general formula for the acoustic-gravity wave dispersion relation, including baroclinicity, rate-of-strain, and all components of the Earth's angular velocity on the Coriolis force. However, we start with (Jones, 2006, equation (10)), which neglects rate of strain in the dispersion relation as a special case of the general dispersion relation.

$$(\mathbf{k}^2+\mathbf{k}_A^2)(N^2-\omega^2)+\mathbf{k}\cdot\mathbf{S}\cdot\mathbf{k}+\mathbf{k}_A\cdot\mathbf{S}\cdot\mathbf{k}_A+\mathbf{A}\cdot\mathbf{k} +1/C^2(\omega^4-4\omega^2\tilde{\mathbf{\Omega}}^2+B^2/2-2i\omega\tilde{\mathbf{\Omega}}\cdot\mathbf{B})=0\,, \quad \text{(A.1)}$$

where N is the Brunt-Väisälä frequency[2], $\mathbf{g}$ is the acceleration due to gravity, $\omega=\sigma-\mathbf{k}\cdot\mathbf{U}$ is the intrinsic frequency, σ is the wave frequency, $\mathbf{U}$ is the background fluid velocity, $\mathbf{k}$ is the wavenumber, $\mathbf{B}$ is the baroclinic vector, $\tilde{\mathbf{\Omega}}=\mathbf{\Omega}+\zeta/4$, where $\zeta=\nabla\times\mathbf{U}$ is vorticity, $\mathbf{\Omega}$ is the Earth's angular velocity, C is sound speed, $\mathbf{k}_A\equiv\nabla\rho/(2\rho)$, where ρ is density, $\mathbf{S}$ is the symmetric matrix defined by

$$S_{\alpha\beta}=\underbrace{-\frac{1}{2\rho}\left(\frac{\partial\tilde{\rho}_{pot}}{\partial x_\alpha}\tilde{g}_\beta+\frac{\partial\tilde{\rho}_{pot}}{\partial x_\beta}\tilde{g}_\alpha\right)}_{1}\underbrace{+4\tilde{\Omega}_\alpha\tilde{\Omega}_\beta}_{2} \underbrace{+\frac{i}{\omega}\left(\tilde{\Omega}_\alpha B_\beta+\tilde{\Omega}_\beta B_\alpha\right)}_{3}\,, \quad \text{(A.2)}$$

$\tilde{\mathbf{g}}\equiv\nabla p/\rho=\mathbf{g}-D\mathbf{U}/Dt-2\mathbf{\Omega}\times\mathbf{U}$ is the effective vector acceleration due to gravity [including (minus) the acceleration of the background flow], $\tilde{\rho}_{pot}$ is local potential density, defined by $\nabla\tilde{\rho}_{pot}=\nabla\rho-\nabla p/C^2$ (Jones, 2005, 2008a), p is pressure,

$$\mathbf{A}=(4\omega\tilde{\mathbf{\Omega}}+i\mathbf{B})\times\mathbf{\Gamma}+2\mathbf{k}_A\cdot\tilde{\mathbf{\Omega}}\mathbf{B}/\omega\,, \quad \text{(A.3)}$$

and $\mathbf{\Gamma}=\mathbf{k}_A-\tilde{\mathbf{g}}/C^2$ is the vector generalization Jones (2001, 2012) of Eckart's coefficient (Gossard and Hooke, 1975, p. 90).

Term 2 in (A.2) is a Coriolis term, which we will be keeping. Term 3 in (A.2) is a baroclinic and Coriolis term, which we shall be neglecting when we neglect baroclinic terms.

Neglecting the baroclinic terms in (A.1), (A.2), and (A.3) gives

$$(\mathbf{k}^2+\mathbf{k}_A^2)(N^2-\omega^2)+\mathbf{k}\cdot\mathbf{S}\cdot\mathbf{k}+\mathbf{k}_A\cdot\mathbf{S}\cdot\mathbf{k}_A+\mathbf{A}\cdot\mathbf{k} +1/C^2(\omega^4-4\omega^2\tilde{\mathbf{\Omega}}^2)=0\,, \quad \text{(A.4)}$$

[2]The Brunt-Väisälä frequency, N, is calculated from $N^2=\nabla\tilde{\rho}_{\rm pot}\cdot\tilde{\mathbf{g}}/\rho=(\nabla\rho-\nabla p/C^2)\cdot\tilde{\mathbf{g}}/\rho$, where $\tilde{\rho}_{\rm pot}$ is local potential density, p is pressure, C is sound speed, $\tilde{\mathbf{g}}=\nabla p/\rho$ is the effective acceleration due to gravity

where $\mathbf{S}$ is the symmetric matrix defined by

$$S_{\alpha\beta}=\underbrace{-\frac{1}{2\rho}\left(\frac{\partial\tilde{\rho}_{pot}}{\partial x_\alpha}\tilde{g}_\beta+\frac{\partial\tilde{\rho}_{pot}}{\partial x_\beta}\tilde{g}_\alpha\right)}_{1}\underbrace{+4\tilde{\Omega}_\alpha\tilde{\Omega}_\beta}_{2}\,, \quad \text{(A.5)}$$

and

$$\mathbf{A}=4\omega\tilde{\mathbf{\Omega}}\times\mathbf{\Gamma}\,. \quad \text{(A.6)}$$

Substituting (A.5) and (A.6) into (A.4) gives

$$(\mathbf{k}^2+\mathbf{k}_A^2)(N^2-\omega^2)-\tfrac{1}{\rho}\mathbf{k}\cdot\nabla\tilde{\rho}_{pot}\,\tilde{\mathbf{g}}\cdot\mathbf{k}-\tfrac{1}{\rho}\mathbf{k}_A\cdot\nabla\tilde{\rho}_{pot}\,\tilde{\mathbf{g}}\cdot\mathbf{k}_A +4(\mathbf{k}\cdot\tilde{\mathbf{\Omega}})^2+4(\mathbf{k}_A\cdot\tilde{\mathbf{\Omega}})^2+4\omega\tilde{\mathbf{\Omega}}\times\mathbf{\Gamma}\cdot\mathbf{k} +1/C^2(\omega^4-4\omega^2\tilde{\mathbf{\Omega}}^2)=0 \quad \text{(A.7)}$$

for the acoustic-gravity-wave dispersion relation in which all components of the Earth's angular velocity are included in the Coriolis terms.

References

Chen, C., Chu, X., McDonald, A. J., Vadas, S. L., Yu, Z., Fong, W., Lu, X., 2013. Inertia-gravity waves in antarctica: A case study using simultaneous lidar and radar measurements at McMurdo/Scott Base (77.8°S, 166.7°E). Journal of Geophysical Research: Atmospheres 118 (7), 2794–2808. URL http://dx.doi.org/10.1002/jgrd.50318

Chen, C., Chu, X., Zhao, J., Roberts, B. R., Yu, Z., Fong, W., Lu, X., Smith, J. A., 2016. Lidar observations of persistent gravity waves with periods of 3-10 h in the Antarctic middle and upper atmosphere at McMurdo (77.83°S, 166.67°E). Journal of Geophysical Research: Space Physics 121 (2), 1483–1502, 2015JA022127. URL http://dx.doi.org/10.1002/2015JA022127

Chu, X., Yu, Z., Gardner, C. S., Chen, C., Fong, W., 2011. Lidar observations of neutral Fe layers and fast gravity waves in the thermosphere (110-155 km) at McMurdo (77.8°S, 166.7°E), antarctica. Geophysical Research Letters 38 (23), L23807. URL http://dx.doi.org/10.1029/2011GL050016

Eckart, C., 1960. Hydrodynamics of Oceans and Atmospheres. Pergamon Press, Oxford.

Gossard, E. E., Hooke, W. H., 1975. Waves in the Atmosphere. Elsevier Scientific Publishing Company, Amsterdam.

Hickey, M., Cole, K., 1987. A quartic dispersion equation for internal gravity waves in the thermosphere. Journal of Atmospheric and Terrestrial Physics 49 (9), 889 – 899, http://dx.doi.org/10.1016/0021-9169(87)90003-1.

Jones, R. M., 2001. The dispersion relation for internal acoustic-gravity waves in a baroclinic fluid. Physics of Fluids 13, 1274–1280, errata available at (Jones, 2012, http://cires.colorado.edu/~mjones/pubs/errata9.pdf, date last viewed 13 May 2016).

Jones, R. M., November 2005. A general dispersion relation for internal gravity waves in the atmosphere or ocean, including baroclinicity, vorticity, and rate of strain. J. Geophys. Res. 110, D22106, doi: 10.1029/2004JD005654, Errata available at (Jones, 2008a, http://cires.colorado.edu/~mjones/pubs/errata7.pdf, date last viewed 13 May 2016).

Jones, R. M., November 2006. Minimum and maximum propagation frequencies for internal gravity waves. J. Geophys. Res. 111, D06109, doi: 10.1029/2005JD006189, Errata available at (Jones, 2008b, http://cires.colorado.edu/~mjones/pubs/errata8.pdf, date last viewed 13 May 2016).

Jones, R. M., 2008a. Errata: A general dispersion relation for internal gravity waves in the atmosphere or ocean, including baroclinicity, vorticity, and rate of strain, *J. Geophys. Res.*, 2005, doi: 10.1029/2004JD005654, Errata available at http://cires.colorado.edu/~mjones/pubs/errata7.pdf (date last viewed 13 May 2016).

Jones, R. M., 2008b. Errata: Minimum and maximum propagation frequencies for internal gravity waves, *J. Geophys. Res.*, 2006, doi: 10.1029/2005JD006189, Errata available at http://cires.colorado.edu/~mjones/pubs/errata8.pdf (date last viewed 13 May 2016).

Jones, R. M., 2012. Errata: The dispersion relation for internal acoustic-gravity waves in a baroclinic fluid, *Physics of Fluids*, 2001, 1274-1280, Errata available at http://cires.colorado.edu/~mjones/pubs/errata9.pdf (date last viewed 13 May 2016).

NRLMSISE-00, Community Coordinated Modeling Center, 2016. NRLMSISE-00 Atmosphere Model, http://ccmc.gsfc.nasa.gov/modelweb/models/nrlmsise00.php.

Phillips, N. A., 1966. The equations of motion for a shallow rotating atmosphere and the "traditional approximation". Journal of the Atmospheric Sciences 23 (5), 626–628, doi:10.1175/1520-0469(1966)023<0626:TEOMFA>2.0.CO;2.
URL http://dx.doi.org/10.1175/1520-0469(1966)023<0626:TEOMFA>2.0.CO;2

Zhao, J., Chu, X., Chen, C., Lu, X., Fong, W., Yu, Z., Jones, R. M., Roberts, B. R., Dörnbrack, A., 2017. Lidar observations of stratospheric gravity waves from 2011 to 2015 at McMurdo (77.84°S, 166.69°E), Antarctica: 1. Vertical wavelengths, periods, and frequency and vertical wave number spectra. Journal of Geophysical Research: Atmospheres 122 (10), 5041–5062, 2016JD026368.
URL http://dx.doi.org/10.1002/2016JD026368